

Study of the neutron-induced fission cross section of ^{237}Np at CERN's n_TOF facility over a wide energy range

A. Stamatopoulos^{1,*}, A. Tsinganis², M. Diakaki^{1,44}, N. Colonna³, M. Kokkoris¹, R. Vlastou¹, A. Kalamara¹, P. Schillebeeckx⁴, L. Tassan-Got⁵, P. Žugec^{6,2}, M. Sabaté-Gilarte^{2,7}, N. Patronis⁸, Z. Eleme⁸, J. Heyse⁴, O. Aberle², J. Andrzejewski⁹, L. Audouin⁵, M. Bacak^{10,2,11}, J. Balibrea¹², M. Barbagallo³, F. Bečvář¹³, E. Berthoumieux¹¹, J. Billowes¹⁴, D. Bosnar⁶, A. Brown¹⁵, M. Caamaño¹⁶, F. Calviño¹⁷, M. Calviani², D. Cano-Ott¹², R. Cardella², A. Casanovas¹⁷, F. Cerutti², Y. H. Chen⁵, E. Chiaveri^{2,14,7}, G. Cortés¹⁷, M. A. Cortés-Giraldo⁷, L. Cosentino¹⁸, L. A. Damone^{3,19}, C. Domingo-Pardo²⁰, R. Dressler²¹, E. Dupont¹¹, I. Durán¹⁶, B. Fernández-Domínguez¹⁶, A. Ferrari², P. Ferreira²², P. Finocchiaro¹⁸, V. Furman²³, K. Göbel²⁴, A. R. García¹², A. Gawlik⁹, S. Gilardoni², T. Glodariu^{†25}, I. F. Gonçalves²², E. González-Romero¹², E. Griesmayer¹⁰, C. Guerrero⁷, F. Gunsing^{11,2}, H. Harada²⁶, S. Heinitz²¹, D. G. Jenkins¹⁵, E. Jericha¹⁰, F. Käppeler²⁷, Y. Kadi², P. Kavrigin¹⁰, A. Kimura²⁶, N. Kivel²¹, I. Knapova¹³, M. Krtička¹³, D. Kurtulgil²⁴, E. Leal-Cidoncha¹⁶, C. Lederer²⁸, H. Leeb¹⁰, J. Lerendegui-Marco⁷, S. Lo Meo^{29,30}, S. J. Lonsdale²⁸, D. Macina², A. Manna^{30,31}, J. Marganec^{9,32}, T. Martínez¹², A. Masi², C. Massimi^{30,31}, P. Mastinu³³, M. Mastromarco³, E. A. Mauger²¹, A. Mazzone^{3,34}, E. Mendoza¹², A. Mengoni²⁹, P. M. Milazzo³⁵, F. Mingrone², A. Musumarra^{18,36}, A. Negret²⁵, R. Nolte³², A. Oprea²⁵, A. Pavlik³⁷, J. Perkowski⁹, I. Porras³⁸, J. Praena³⁸, J. M. Quesada⁷, D. Radeck³², T. Rauscher^{39,40}, R. Reifarth²⁴, C. Rubbia², J. A. Ryan¹⁴, A. Saxena⁴¹, D. Schumann²¹, P. Sedyshev²³, A. G. Smith¹⁴, N. V. Sosnin¹⁴, G. Tagliente³, J. L. Tain²⁰, A. Tarifeño-Saldivia¹⁷, S. Valenta¹³, G. Vannini^{30,31}, V. Variale³, P. Vaz²², A. Ventura³⁰, D. Vescovi^{3,42}, V. Vlachoudis², A. Wallner⁴³, S. Warren¹⁴, C. Weiss¹⁰, P. J. Woods²⁸, and T. Wright¹⁴
and the n_TOF Collaboration

¹National Technical University of Athens, Greece

²European Organization for Nuclear Research (CERN), Switzerland

³Istituto Nazionale di Fisica Nucleare, Sezione di Bari, Italy

⁴European Commission, Joint Research Centre, Geel, Retieseweg 111, B-2440 Geel, Belgium

⁵Institut de Physique Nucléaire, CNRS-IN2P3, Univ. Paris-Sud, Université Paris-Saclay, F-91406 Orsay Cedex, France

⁶Department of Physics, Faculty of Science, University of Zagreb, Zagreb, Croatia

⁷Universidad de Sevilla, Spain

⁸University of Ioannina, Greece

⁹University of Lodz, Poland

¹⁰Technische Universität Wien, Austria

¹¹CEA Irfu, Université Paris-Saclay, F-91191 Gif-sur-Yvette, France

¹²Centro de Investigaciones Energéticas Medioambientales y Tecnológicas (CIEMAT), Spain

¹³Charles University, Prague, Czech Republic

¹⁴University of Manchester, United Kingdom

¹⁵University of York, United Kingdom

¹⁶University of Santiago de Compostela, Spain

¹⁷Universitat Politècnica de Catalunya, Spain

¹⁸INFN Laboratori Nazionali del Sud, Catania, Italy

¹⁹Dipartimento di Fisica, Università degli Studi di Bari, Italy

²⁰Instituto de Física Corpuscular, CSIC - Universidad de Valencia, Spain

²¹Paul Scherrer Institut (PSI), Villigen, Switzerland

²²Instituto Superior Técnico, Lisbon, Portugal

²³Joint Institute for Nuclear Research (JINR), Dubna, Russia

²⁴Goethe University Frankfurt, Germany

²⁵Horia Hulubei National Institute of Physics and Nuclear Engineering, Romania

²⁶Japan Atomic Energy Agency (JAEA), Tokai-mura, Japan

²⁷Karlsruhe Institute of Technology, Campus North, IKP, 76021 Karlsruhe, Germany

²⁸School of Physics and Astronomy, University of Edinburgh, United Kingdom

²⁹Agenzia nazionale per le nuove tecnologie (ENEA), Bologna, Italy

³⁰Istituto Nazionale di Fisica Nucleare, Sezione di Bologna, Italy

³¹Dipartimento di Fisica e Astronomia, Università di Bologna, Italy

³²Physikalisch-Technische Bundesanstalt (PTB), Bundesallee 100, 38116 Braunschweig, Germany

³³Istituto Nazionale di Fisica Nucleare, Sezione di Legnaro, Italy

³⁴Consiglio Nazionale delle Ricerche, Bari, Italy

³⁵Istituto Nazionale di Fisica Nucleare, Sezione di Trieste, Italy

³⁶Dipartimento di Fisica e Astronomia, Università di Catania, Italy

³⁷University of Vienna, Faculty of Physics, Vienna, Austria

³⁸University of Granada, Spain

³⁹Department of Physics, University of Basel, Switzerland

⁴⁰Centre for Astrophysics Research, University of Hertfordshire, United Kingdom

⁴¹Bhabha Atomic Research Centre (BARC), India

⁴²Istituto Nazionale di Fisica Nucleare, Sezione di Perugia, Italy

⁴³Australian National University, Canberra, Australia

⁴⁴CEA, Cadarache, DEN/DER/SPRC/LEPh, 13108 Saint Paul Les Durance, France

Abstract. Neutron-induced fission cross sections of isotopes involved in the nuclear fuel cycle are vital for the design and safe operation of advanced nuclear systems. Such experimental data can also provide additional constraints for the adjustment of nuclear model parameters used in the evaluation process, resulting in the further development of fission models. In the present work, the $^{237}\text{Np}(n,f)$ cross section was studied at the EAR2 vertical beam-line at CERN's n_TOF facility, over a wide range of neutron energies, from meV to MeV, using the time-of-flight technique and a set-up based on Micromegas detectors, in an attempt to provide accurate experimental data. Preliminary results in the 200 keV – 14 MeV neutron energy range as well as the experimental procedure, including a description of the facility and the data handling and analysis, will be presented.

1 Introduction

^{237}Np is the most abundant minor actinide produced in current nuclear power plants. In addition, the neutron-induced fission cross section of ^{237}Np has a high value and it is frequently used as a reference reaction in measurements on account of its low fission threshold and moderate activity. This importance is reflected in the High Priority Request List [1] in which the $^{237}\text{Np}(n,f)$ cross section is included since 2015 with 2 – 3% target accuracies in the energy region between 200 keV and 20 MeV [2]. In addition neptunium can be used in explosive devices, therefore a monitoring scheme was approved by the IAEA to keep track of separated ^{237}Np [3]. An efficient means to minimise its proliferation includes its use as nuclear fuel in fast reactors, thus further increasing the importance of $^{237}\text{Np}(n,f)$ cross section studies. In this respect about 50 measurements have been reported in the EXFOR database [4] since 1947, three of which were performed the last decade at n_TOF (Paradela et al. [5], Diakaki et al. [6]) and at NCSR “Demokritos” (Diakaki et al. [7, 8]) and were found to be 7% discrepant in the 1 – 5 MeV energy region. In an attempt to resolve the discrepancies, the $^{237}\text{Np}(n,f)$ reaction was studied at the 19.5 m vertical flight path, referred to as EAR2, at the n_TOF facility at CERN, in the energy regime between 200 keV and 14 MeV.

2 Experimental setup

2.1 EAR2 at the n_TOF facility

The study of the $^{237}\text{Np}(n,f)$ reaction was performed at the n_TOF facility at CERN [9], in the second experimental area, commonly referred to as EAR2 [10], that features a 19.5 m flight-path. The neutron spectrum of EAR2, which spans from the meV to the MeV region, is produced by spallation reactions induced by a 20 GeV/c pulsed proton beam, delivered by CERN's Proton Synchrotron, that impinges on a 40 cm in length and 60 cm in diameter lead

block. The wide neutron energy spectrum in combination with the high instantaneous flux allows the study of high-activity and/or low-mass samples in a broad energy range as previous measurements showed [11, 12]. Therefore it was considered as a suitable apparatus to study the $^{237}\text{Np}(n,f)$ from subthreshold energies up to the second chance fission threshold.

2.2 Fission foils

To study the $^{237}\text{Np}(n,f)$ reaction four fission foils in the chemical form of neptunium hydroxide (H_5NpO_5), with 1.79 mg total mass and an average areal density of the order of $6.4 \times 10^{-5} \text{ g/cm}^2$ were prepared at JRC-Geel. An additional sample prepared at IPN-Orsay was also provided in order to study systematic effects due to the sample itself. The mass of this sample was 1.48 mg and its areal density $2.7 \times 10^{-4} \text{ g/cm}^2$.

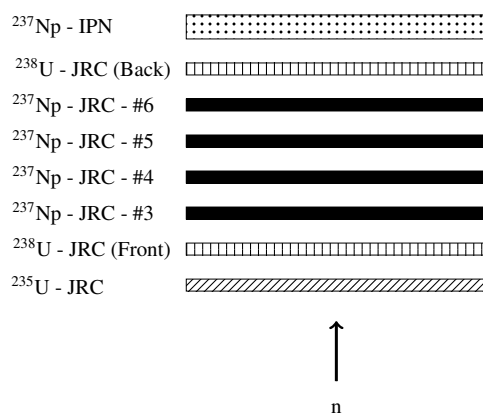


Figure 1. Schematic view of the fission foils stack, with respect to the neutron beam direction.

Apart from the neptunium samples, three reference foils also prepared at JRC-Geel in the form of uranium hydroxide ($\text{H}_6\text{O}_6\text{U}$) were used: (a) a ^{235}U sample with a

*e-mail: athanasios.stamatopoulos@cern.ch

mass of 0.51 mg and an areal density of 7.2×10^{-5} g/cm² and (b) two ²³⁸U samples with a total mass of 2.76 mg and an average areal density of 2.7×10^{-4} g/cm². A schematic representation of the position of each fission foil with respect to the incident neutron beam, is shown in fig. 1.

2.3 Detectors

The measurement was performed using a set-up based on the compact, low mass Micromegas (MicroMesh Gaseous Structure) detector [13] whose volume is divided into two parts by a thin conductive micromesh: the drift region (5 mm) and the narrow amplification region (50 μm). Typical electric fields applied in the drift region, which lies between the cathode and the micromesh, are of the order of 1 kV/cm. The amplification region is made of a 50 μm thick and 9.5 cm in diameter Kapton foil and lies between the micromesh and the anode of the detector. Typical electric fields applied in this region are of the order of 50 kV/cm, thus causing the formation of a relatively strong signal through avalanche multiplication. The detectors and samples were housed in a cylindrical aluminium chamber which was filled with an Ar:CF₄:iC₄H₁₀ gas mixture at 88:10:2% volume fraction, at atmospheric pressure.

2.4 Data acquisition

The detector signals were recorded by a digital acquisition system [14], operating at a sampling rate of 225 MHz, with a resolution of 12-bits and an acquisition window which had a length of 16 ms. To minimize the amount of data recorded during the acquisition, a zero-suppression algorithm was applied, therefore short time-traces are stored for the subsequent analysis.

3 Data reduction and analysis

Data at n_TOF is processed off-line through the use of a pulse shape analysis framework, in which the signal recognition was based on the calculation of the first derivative [15]. For each identified signal, the corresponding attributes (amplitude, time-of-flight, area etc.) were stored in list-mode files which were then processed to calculate the reaction yield.

Prior to the cross section calculation various correction factors had to be applied, in order to take the following effects into account:

- Counting losses due to high counting rates or inefficient use of the reconstruction routine.
- Rejection of low amplitude fission signals due to the application of an amplitude threshold. This threshold was applied in order to reject α-particle signals originating from the radioactivity of the samples.
- Parasitic counts that contributed to the recorded yield and were attributed to fission reactions from contaminants or impurities present in the fission foils.
- Self-absorption of fission fragments within the fission foils.

- Neutron beam attenuation in the various material layers of the detector-sample stacks.
- Spontaneous fission events.
- Cluster decay events.
- Parasitic counts from photofission events that contributed to the recorded fission yield.

3.1 Dead-time correction

The most important effect in the 200 keV – 14 MeV region was the counting losses due to the high counting rates from the massive ²³⁷Np sample provided by IPN-Orsay. To illustrate this effect, the ²³⁷Np(n,f) cross section is calculated for two different samples: (a) a light one, prepared at JRC-Geel and (b) the heavy one provided by IPN-Orsay. Both cross sections, seen in fig. 2, were corrected in terms of pile-up by using the methodology proposed by Coates [16]. It is evident that the heavier sample suffered significant counting losses since the reaction rate was appreciably higher by a factor of 3.5 compared to the corresponding one of the low mass sample. To correct for the significant amount of counting losses, which reached 40%, the methodology proposed in [17] was applied which yielded a cross section that was compatible within less than 5% with respect to the ones calculated from the low mass samples.

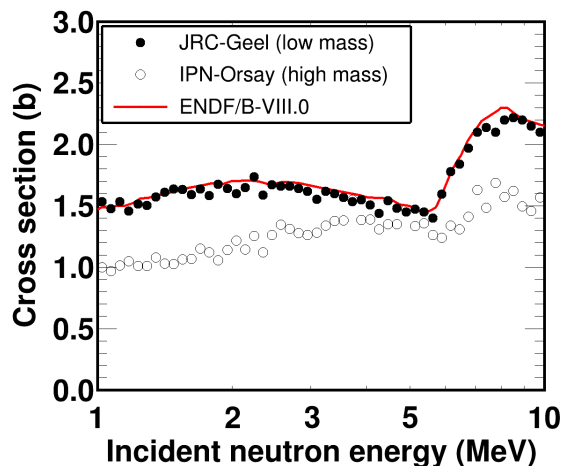


Figure 2. The sample provided by IPN-Orsay was 3.5 times heavier than the corresponding ones from JRC-Geel. The effect of the counting losses is quite visible in the cross section.

3.2 Validation of the analysis

The accurate calculation of the cross section of a reference reaction, such as the ²³⁸U(n,f) one, is a validation test of the analysis procedure. In the present case, the ²³⁸U(n,f) cross section was derived from both ²³⁸U targets, relative to ²³⁵U(n,f). As shown in fig. 3, the reference ²³⁸U(n,f) cross section was adequately reproduced up to 14 MeV, within less than 3%, compared to the ENDF/B-VIII.0 evaluation.

4 Preliminary results

The ²³⁷Np(n,f) cross section was derived by calculating the weighted average between the individual cross sections

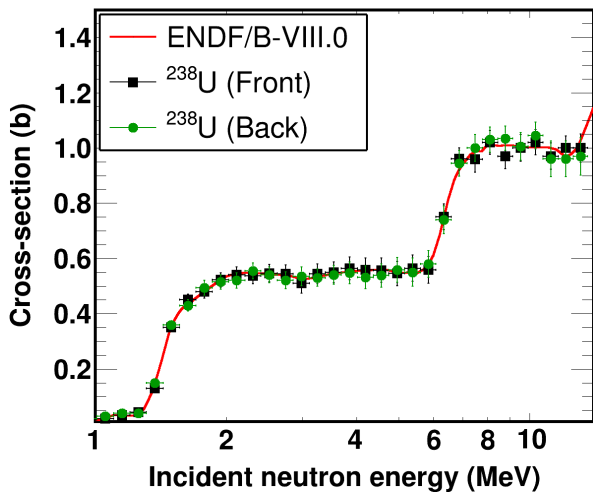


Figure 3. The ENDF/B-VIII.0 $^{238}\text{U}(n,f)$ cross section was adequately reproduced from both ^{238}U samples up to 14 MeV.

obtained from three neptunium samples, provided by JRC-Geel and the one provided by IPN-Orsay, with reference to the $^{235}\text{U}(n,f)$ reaction. The preliminary results covered an energy region between 200 keV and 14 MeV, as can be seen in fig. 4. The present dataset is in agreement with the measurement by Diakaki et al. [6], in the region above 1 MeV, where discrepancies of the order of 7% were observed with the measurement by Paradela et al. [5] thus confirming the most recent n_TOF results. The data for lower energies along with the corresponding ones for the fourth target from JRC-Geel are currently under analysis.

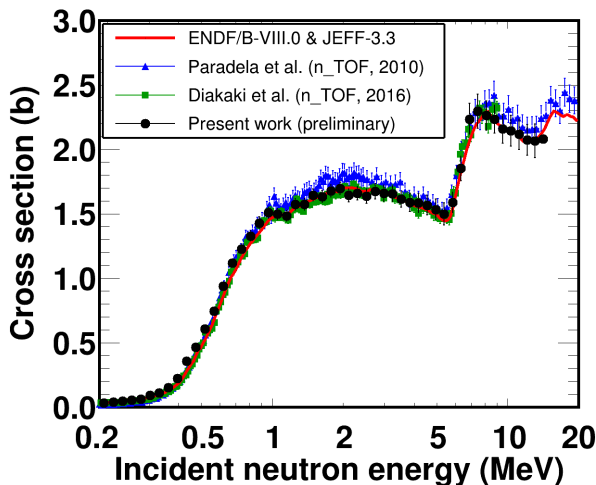


Figure 4. The preliminary $^{237}\text{Np}(n,f)$ cross section that was derived from three samples provided by JRC-Geel and the IPN-Orsay one, is in agreement with the cross section reported by Diakaki et al. [6].

Acknowledgements

This research is implemented through IKY scholarships programme and co-financed by the European Union (European Social Fund - ESF) and Greek national funds through the action entitled Reinforcement of Postdoctoral Researchers, in the framework of the Operational Programme Human Resources Development Program, Education and Lifelong Learning of the National Strategic Reference Framework (NSRF) 2014–2020.

References

- [1] E. Dupont, et al., *These proceedings. The High Priority Request List (HPRL). The HPRL database is available online at <https://www.oecd-nea.org/dbdata/hprl/>*
- [2] *High priority request ID 44 : $^{237}\text{Np}(n,f)$* , <https://www.oecd-nea.org/dbdata/hprl/hprlview.pl?ID=464>
- [3] *Safeguards Implementation Practices Guide on Provision of Information to the IAEA (IAEA-SVS-33)* (2016), https://www-pub.iaea.org/MTCD/Publications/PDF/SVS_33_web.pdf
- [4] N. Otuka, et. al., Nucl. Data Sheets **120**, 272 (2014)
- [5] C. Paradela, for the n_TOF Collaboration, Phys. Rev. C **82**, 034601 (2010)
- [6] M. Diakaki, for the n_TOF Collaboration, Phys. Rev., C **93**, 034614 (2016)
- [7] M. Diakaki, et al., Europ. Phys. J. A **49**, 62 (2013)
- [8] M. Diakaki, et al., Nucl. Data Sheets **119**, 52 (2014)
- [9] C. Rubbia, et al., Tech. Rep. CERN-LHC-98-002-EET-Add.1, CERN (1998), <https://cds.cern.ch/record/363828>
- [10] C. Weiss, et al., Nucl. Instrum. Meth. A **799**, 90 (2015)
- [11] M. Barbagallo, et al, Phys. Rev. L. **117**, 152701 (2016)
- [12] A. Stamatopoulos, et al., EPJ Web of Conferences **146**, 04030 (2017)
- [13] S. Andriamonje, et. al., Journal of the Korean Physical Society **59**, 1601 (2011)
- [14] U. Abbondanno, et al., Nucl. Instrum. Meth. A **538**, 692 (2005)
- [15] P. Žugec, et al., Nucl. Instrum. Meth. A **812**, 134 (2016)
- [16] P.B. Coates, J. Phys. E **5**, 148 (1972)
- [17] A. Stamatopoulos, et al., Nucl. Inst. Meth A **913**, 40 (2019)